J. Eng. Technol. Sci., Vol. 54, No. 4, 2022, 220411

Strength Enhancement, Ductility, and Confinement Effectiveness Index of Fly Ash-based Geopolymer Concrete Square Columns

Herwani[1,2,*], Iswandi Imran[1], Bambang Budiono[1] & Ediansjah Zulkifli[1]

[1]Department of Civil Engineering, Faculty of Civil and Environmental Engineering, Institut Teknologi Bandung, Jalan Ganesa No. 10, Bandung 40132, Indonesia
[2]Department of Civil Engineering, Faculty of Engineering, University of Tanjungpura, Jalan Prof. Hadari Nawawi, Pontianak 78124, Indonesia
*E-mail: herwani@civil.untan.ac.id

Highlights:

- Investigation of the performance of a geopolymer concrete square column.
- Formulation of confined concrete peak stress (f'_{cc}) was developed.
- Formulation of strength enhancement (K) was developed.
- Discussion of the effect of tie spacing and f'_c on the strength enhancement, ductility, and confinement effectiveness index.
- Comparison of strength enhancement of confined concrete equations.

Abstract. Geopolymer concrete is an environmentally friendly construction material that has the potential to be applied in building structures. It is important to understand the structural behavior of geopolymer concrete. This paper presents an experimental investigation into the performance of structural elements of geopolymer concrete under concentric axial loads. The specimens were twelve square columns with a size of 170 x 170 mm and a height of 480 mm. The study variables were the tie spacing and the compressive strength of unconfined geopolymer concrete (f'_c). The test results showed that the increase in f'_{cc} was not as significant as the increase in unconfined concrete compressive strength (f'_c). The value of strength enhancement (K) tended to decrease. The column ductility (μ) and confinement effectiveness index (I_c) had optimum values. The effect of increasing the tie spacing (s) decreased the K, I_c, and μ values of the column. The proposed f'_{cc} formulation for geopolymer concrete is compatible.

Keywords: *compressive strength; fly ash; geopolymer concrete; square column; tie spacing.*

1 Introduction

Geopolymer concrete is a kind of concrete that does not use Portland cement (PC) [1,2]. Geopolymer paste is used as binder of coarse aggregates, fine aggregates, and other unreacted materials. The manufacture of geopolymer concrete is carried

Received May 28th, 2021, 1st Revision November 11th, 2021, 2nd Revision January 31st, 2022, Accepted for publication March 15th, 2022.
 ISSN: 2337-5779,
DOI: 10.5614/j.eng.technol.sci.2022.54.4.11

out using common concrete technology methods [3]. Geopolymer paste is produced by polymerizing aluminosilicates, such as fly ash, metakaolin, slag, rice husk ash, and high calcium wood ash, through activation using an alkaline solution. Hence, the efficiency in producing geopolymer concrete is highly dependent on the activators as well as the type of aluminosilicate source [4,5]. A recent study of cement material by Balamuralikrishnan and Saravanan [6] used a new ultrafine material called Alccofine (AF), which is manufactured from glass waste for the replacement of cement.

Ganesan, *et al.* [7] investigated 36 confined concrete cylinders, of which 24 were made from geopolymer concrete (GPC) and the rest from cement-based concrete (PCC). The experimental results showed that the strength of the confined GPC concrete was greater than that of the PCC concrete. Another test was carried out on square GPC column elements added with steel fiber reinforcement [8]. The investigation results showed that the GPC column behaved similarly to the PCC column. Muslikh, *et al.* [9] conducted tests on confined GPC concrete with parameter analysis of hoop spacing, volumetric ratios of reinforcement, and yield stress of hoops. The test results showed that the strength enhancement and deformability of the GPC concrete were better than that of the PCC concrete. Sumajouw, *et al.* [10] and Rahman, *et al.* [11] conducted experiments on slender columns with a square cross-section using low calcium fly ash-based geopolymer concrete. The experimental results showed that the GPC column had a higher axial load-bearing capacity and better ductility than the PCC column. Similar results were obtained by Sujatha, *et al.* [12] in a study on a GPC slender column with a circular cross-section. Nhabih, *et al.* [13] studied the structural behavior of eccentrically loaded GFRP reinforced columns made of geopolymer concrete. Seven short square columns were tested. The study results showed that under large eccentricity, reinforcement of a geopolymer concrete column by GFRP bars had an outstanding effect on the column's ultimate load capacity. It is necessary to study the effect of GFRP reinforcements on the behavior of geopolymer concrete structural elements under sustained loads. Nguyen, *et al.* [14] investigated the long-term deflection of hybrid GFRP/steel reinforced concrete beams under sustained loads. The experimental results showed that tensile steel reinforcements in hybrid GFRP/steel RC beams significantly reduced the immediate deflection.

The use of tight spiral reinforcement spacing on a circular column can produce almost uniform passive lateral pressure, while stirrups in square columns tend to produce non-uniform passive lateral pressure [15-17]. The effectiveness of confinement also differs between spiral reinforcement and stirrups. The highest lateral pressure of a square column is at the corners and points of the crossties [16]. Studies on the compressive strength of confined concrete (f'_{cc}), strength enhancement, ductility, and the confinement effectiveness index of rectangular confined geopolymer concrete columns are still rare. Therefore, this paper studied the performance of square GPC columns under concentric axial loads.

2 Experimental Programs

2.1 Materials

Low-calcium fly ash obtained from the Suralaya Coal-Fired Power Plant in Banten was used as the raw material. It was classified as class F fly ash according to the ASTM C618-15 standard [18]. The chemical composition of the fly ash from the XRF analysis results is presented in Table 1.

Table 1 The chemical composition of Suralaya fly ash (in % of weight).

Fly Ash	SiO_2	Al_2O_3	Fe_2O_3	CaO	MgO	TiO2	Na_2O	K_2O	SO_3	LoI*
SF2**	52.51	23.77	8.98	7.32	3.50	0.66	0.74	0.61	0.29	0.31

*Loss on ignition ** Suralaya Fly-Ash 2

Sodium hydroxide (NaOH) 8M solution and sodium silicate (Na_2SiO_3) solution were used as alkaline activators. To increase the workability of the fresh concrete, a commercially available high-range water-reducing admixture based on naphthalene was used. Fine aggregate and coarse aggregate were taken from a local quarry. The size of the coarse aggregate was determined by passing through a 20-mm and a 10-mm sieve. Longitudinal reinforcement used 10-mm deformed bars (fy = 392.35 Mpa, while lateral reinforcement used 8-mm plain bars (fy = 460.65 Mpa).

The mixture proportions used can be seen in Table 2. Concrete mixing is done using a pan mixer for approximately 5 to 10 minutes at a speed of 25 rpm.

Table 2 Mixture proportions of geopolymer concrete.

Materials	M 30	M 25	M 20
Coarse aggregate (SSD)	1200	1142.7	1224.4
Dia. 4.5-9.5 mm	540	457.1	489.8
Dia. 9.5-19.5 mm	660	685.6	734.7
Fine aggregate (SSD)	600	521.8	587.8
Fly ash	450	410	408
NaOH solutions (8 Mol)	80	110	85
Na_2SiO_3 solutions	120	120	8.2
Superplasticizer	9	8.2	8.2
Added water	-	2.3	9.8
Compressive strength *fc'* (Mpa)	37.87	30.45	26.2

2.2 Specimen Details and Instrumentation

In this study, a total of twelve square column specimens were tested. The cross-section of the columns was 170 x 170 mm and had a height of 480 mm. There were three columns of plain concrete and nine columns of reinforced concrete. To determine the strain on the stirrup, four FLA strain gauge types were installed, as shown in Figure 1. Two other strain gauges (SG5 and SG6) were attached to the longitudinal reinforcement to observe the strain due to axial deformation of the column. Stirrups were used as lateral reinforcement according to the design standards for earthquake-resistant structures. The spacing was set at 30 mm, 50 mm, and 70 mm.

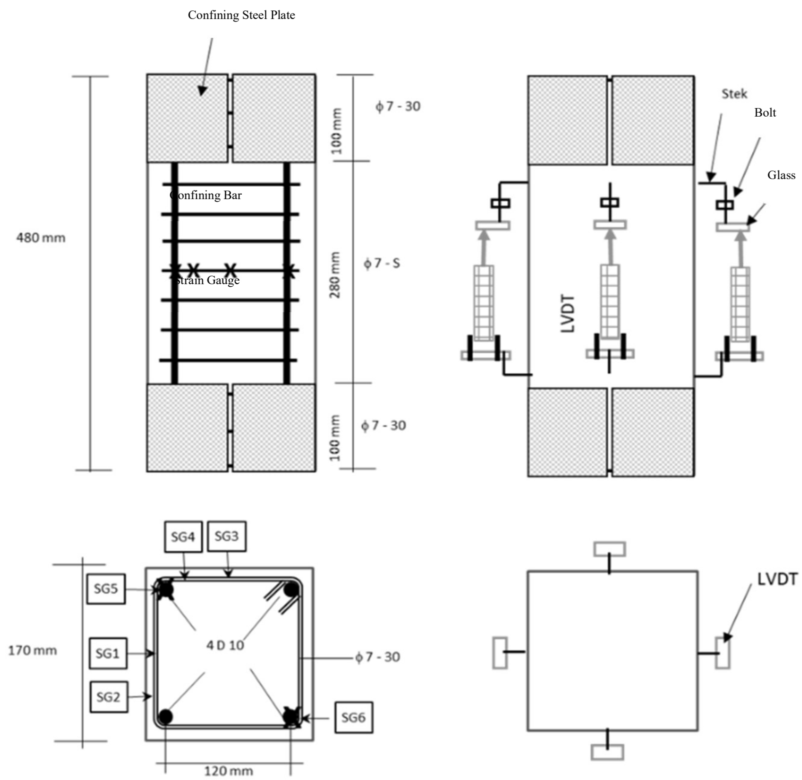

Figure 1 Test specimen and instrumentation.

2.3 Test Procedure

All specimens were tested on a Universal Test Machine (UTM) with a load capacity of 2000 kN. Each side of the column was installed with linear variable differential transducers (LVDT) to measure the axial deformation (Figure 2). In addition, two LVDTs were placed in the middle of the study area to determine the lateral deformation of the column. Loading was carried out until the load decreased significantly. All test data, such as reinforcement strain, axial deformation, and axial load, were recorded on a computer system and in a data logger.

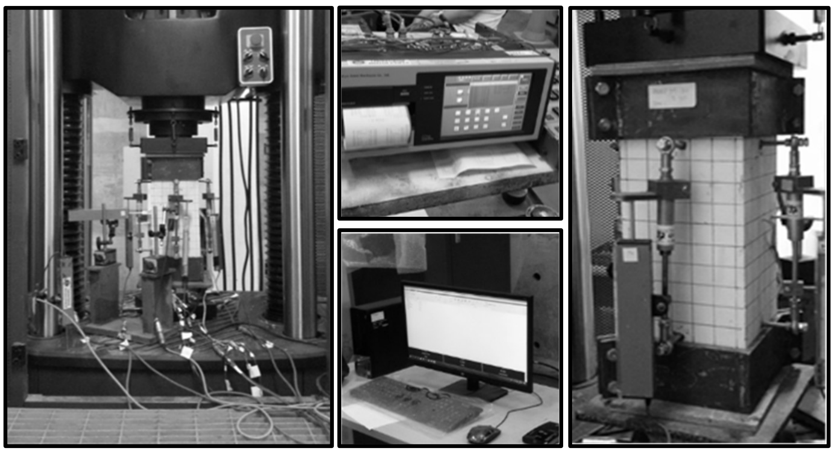

Figure 2 Test set-up, data logger, monitor, and specimen.

2.4 Strength Enhancement, Ductility, and Confinement Effectiveness Index Computation

The strength enhancement of the column was obtained from the ratio of confined concrete compressive strength (f'_{cc}) to unconfined concrete compressive strength (f'_{co}), as shown in Eq. (1) [19]:

$$K = \frac{f'_{cc}}{f'_{co}} \tag{1}$$

The column ductility was obtained using Eq. (2) proposed by Saatcioglu and Razvi [20]:

$$\mu = \frac{\varepsilon_{85}}{\varepsilon_1} \tag{2}$$

The confinement effectiveness index was calculated based on Eq. (3) proposed by Paultre and Legeron [21]:

$$Ic = \frac{f_{le}}{f'_{co}} \tag{3}$$

The effective lateral pressure f_{le} was obtained based on Eq. (4):

$$f_{le} = k_e f_l = k_e \frac{A_{sh} f_{sh}}{S h_c} \tag{4}$$

The coefficient of confinement geometric effectiveness k_e was calculated by the Eqs. (5) & (6):

$$k_e = \frac{\left(1-\sum_{i=1}^{n}\frac{(w_i)^2}{6 b_c d_c}\right)\left(1-\frac{s'}{2b_c}\right)\left(1-\frac{s'}{2d_c}\right)}{(1-\rho_{cc})} \tag{5}$$

$$\rho_{cc} = \frac{A_{sl}}{A_c} \tag{6}$$

3 Results and Discussion

3.1 Experimental Results

A summary of the axial capacity, compressive strength, and axial strain of the columns is presented in Table 3, while the collapse pattern of the specimens is shown in Figure 3. In general, all specimens were subjected to shear cone failure due to a combination of axial compressive and lateral forces. The presence of lateral force is a reaction to the lateral expansion of the confined concrete core. For the specimen with s = 30 mm, at the end of the test it was seen that the core of the column could be properly confined (Figure 3(b). From the top to the bottom of the study area, the cross-section area of confined concrete was the same. Meanwhile, for the specimens with s = 50 mm and s = 70 mm, the cross-section area of the middle study area had decreased due to breaking of the concrete core (Figure 3(c) and 3(d)). These results indicate that increasing s can decrease the column axial capacity. Based on the ratio of $P_{max}/P_o \geq 1$, as shown in Table 3, the column with $\rho_s/\rho_{ACI} = 0.5$ fulfilled the design capacity. Thus, the required ratio of lateral reinforcement for concentric axial load design is $\rho_s = 0.5\ \rho_{ACI}$.

Table 3 Summary of test results.

Specimen	ϕ-Spacing	$\rho_s = A_{sl}/s.h_c$ (%)		P_o	P_{max}	ε_l	ε_{85}	f'_{co}	f'_{cc}	$f'_{cc}/$	$P_{max}/$	$\rho_{exp}/$	$\varepsilon_{85}/\varepsilon_1$
	(mm)	ACI/SNI	Exp.	(kN)	(kN)			(Mpa)	(Mpa)	f'_{co}	P_o	ρ_{ACI}	
AKKP-M20-S30	7.45 - 30	1.33	2.25	816.10	1040.50	0.0036	0.0391	24.57	36.00	1.47	1.27	1.69	10.81
AKKP-M20-S50	7.45 - 50	1.33	1.35	816.10	937.13	0.0028	0.0156	24.57	32.43	1.32	1.15	1.01	5.61
AKKP-M20-S70	7.45 - 70	1.33	0.96	816.10	894.45	0.0020	0.0091	24.57	30.80	1.25	1.10	0.72	4.47
AKKP-M25-S30	7.45 - 30	1.55	2.25	897.82	1126.76	0.0033	0.0348	27.42	38.99	1.42	1.25	1.45	10.55
AKKP-M25-S50	7.45 - 50	1.55	1.35	897.82	1015.53	0.0027	0.0184	27.42	35.14	1.28	1.13	0.87	6.72
AKKP-M25-S70	7.45 - 70	1.55	0.96	897.82	985.47	0.0021	0.0109	27.42	34.10	1.24	1.10	0.62	5.24
AKKP-M30-S30	7.45 - 30	1.93	2.25	1062.16	1301.60	0.0038	0.0296	33.17	45.04	1.36	1.23	1.17	7.82
AKKP-M30-S50	7.45 - 50	1.93	1.35	1062.16	1178.16	0.0033	0.0155	33.17	40.77	1.23	1.11	0.70	4.72
AKKP-M30-S70	7.45 - 70	1.93	0.96	1062.16	1147.31	0.0027	0.0108	33.17	39.70	1.20	1.08	0.50	4.03

(a) (b) (c) (d)

Figure 3 The collapse pattern of geopolymer concrete column specimens with stirrup spacing ***s***: (a) plain column, (b) ***s* = *30 mm***, (c) *s = 50 mm*, (d) *s =70 mm*.

3.2 Discussion

3.2.1 Effect of Compressive Strength

The effect of concrete compressive strength on strength enhancement, ductility, and confinement effectiveness index can be seen in Table 4.

Table 4 Strength enhancement, ductility, and confinement effectiveness index of geopolymer concrete columns.

Specimen	ϕ-Spacing (mm)	*At Max Load (P_{max}) (Mpa)*				f'_{co} (Mpa)	f'_{cc} (Mpa)	*K*	μ	*Ic* (%)
		ε_{Transv}	f_{sh}	f_l	f_{le}					
AKKP-M20-S30	7.45 - 30	0.0021	439.77	9.89	4.84	24.57	36.00	1.47	10.81	19.68
AKKP-M25-S30	7.45 - 30	0.0025	460.65	10.36	5.07	27.42	38.99	1.42	10.55	18.47
AKKP-M30-S30	7.45 - 30	0.0033	460.65	10.36	5.07	33.17	45.04	1.36	7.82	15.27
AKKP-M20-S50	7.45 - 50	0.0017	353.08	4.77	1.95	24.57	32.43	1.32	5.61	7.92
AKKP-M25-S50	7.45 - 50	0.0020	418.48	5.65	2.31	27.42	35.14	1.28	6.72	8.41
AKKP-M30-S50	7.45 - 50	0.0027	460.65	6.22	2.54	33.17	40.77	1.23	4.72	7.65
AKKP-M20-S70	7.45 - 70	0.0015	318.45	3.07	1.03	24.57	30.80	1.25	4.47	4.19
AKKP-M25-S70	7.45 - 70	0.0019	393.15	3.79	1.27	27.42	34.10	1.24	5.24	4.63
AKKP-M30-S70	7.45 - 70	0.0026	460.65	4.44	1.49	33.17	39.70	1.20	4.03	4.48

Strength enhancement K decreases with an increase of concrete compressive strength. The decrease of K in the AKKP-M25-S30 and AKKP-M30-S30 columns against the AKKP-M20-S30 was 5% and 11%, respectively. A similar decrease also occurred in the AKKP-M25-S50, AKKP-M30-S50, AKKP-M25-S70, AKKP-M30-S70 columns, by 4%, 9%, and 1%, 5%, respectively. Different phenomena were seen in ductility μ and confinement effectiveness index *Ic*. The columns with $A_{sh} < A_{sh\ ACI}$ reached the optimum value for M25 concrete quality. Meanwhile, the column with $A_{sh} > A_{sh\ ACI}$ gradually decreased in ductility and index of confinement effectiveness (Figure 5). The compatibility of concrete and reinforcing steel as well as the configuration of the reinforcing bars contribute to achieving optimum ductility and index of confinement effectiveness.

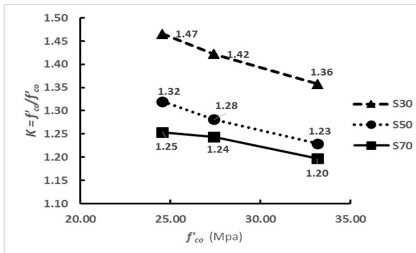

(a)

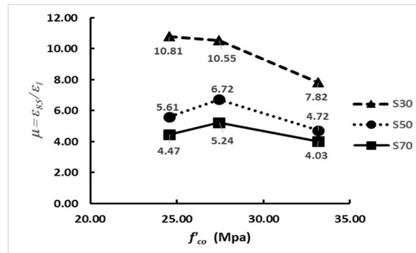

(b)

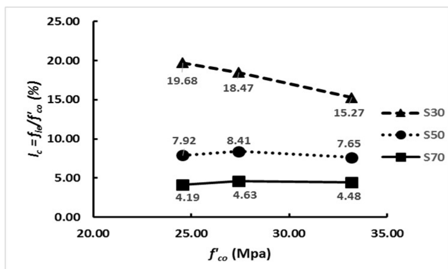

(c)

Figure 4 The effect of GPC compressive strength *f'co* on the behavior of the AKKP specimens: (a) strength enhancement K, (b) ductility μ, (c) confinement effectiveness index I_c

In general, the effect of concrete compressive strength used in the column structural elements can increase the confined concrete strength f'_{cc} but reduces the strength enhancement *K*, ductility μ, and the confinement effectiveness index I_c.

3.2.1 Effect of Tie Spacing

Tie spacing affects the strength enhancement, ductility, and confinement effectiveness index. Increasing the tie spacing *S* causes a decrease in the strength of confined concrete f'_{cc}. The ability of the ties to stem concrete lateral expansion becomes ineffective. The lateral force due to concrete core expansion is not fully resisted by tie reinforcement, causing buckling of the longitudinal reinforcement and concrete crushing. Thus, the strength enhancement *K* is also reduced. Based on Figure 5(a), the value of *K* for AKKP-M20-S70 ($\rho_s = 0.96$) was 1.25. This means that the addition of the lateral reinforcement with $\rho_s = 0.96$ was able to increase f'_{cc} by 25% f'_{co}. The highest increase in confined concrete strength f'_{cc} was achieved in AKKP-M20-S30, which was 47% ($K = 1.47$). The lowest increase was 20% ($K = 1.2$) in AKKP-M30-S70. In general, with every addition of $\rho_s = 1\%$ there was an increase in f'_{cc} by 20%.

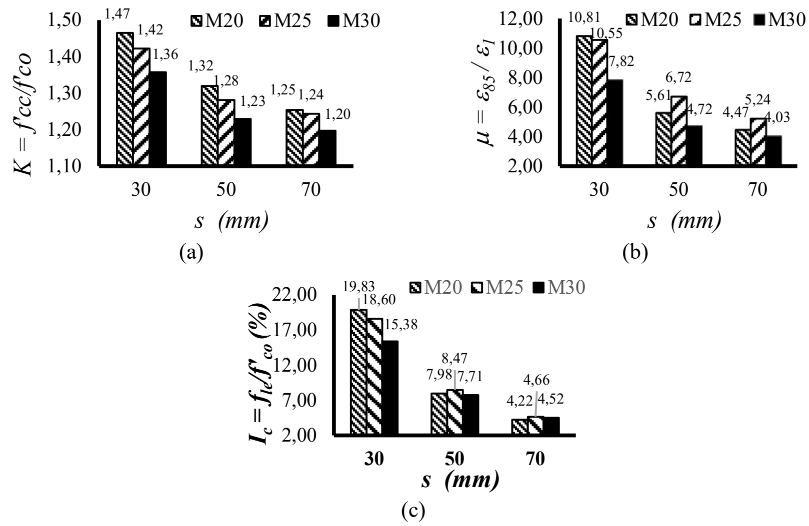

Figure 5 The effect of tie spacing S on the behavior of the AKKP specimens: (a) strength enhancement K, (b) ductility μ, (c) confinement effectiveness index I_c.

As an analog of the K value, increasing the tie spacing S decreases the ductility μ and the confinement effectiveness index I_c (Figures 5(b) and 5(c)). Each addition of $S = 20$ mm could reduce the column ductility by 15% to 48%. Column ductility also indicates the effectiveness of confinement. The higher the column ductility, the higher the effectiveness of confinement. This is indicated by the value of the confinement effectiveness index, *Ic*. The column with the largest ductility produced the highest percentage (19.68%).

3.2.2 Development of Compressive Strength Model for Confined Geopolymer Concrete Square Columns

In general, the mechanical properties of geopolymer concrete are similar to those of conventional concrete based on Portland cement [1]. In this paper, the development was carried out based on the concept proposed by Saatcioglu & Razvi [16], which is based on a model developed by Richart, *et al.* [22]. The general equation for the compressive strength of confined concrete is $f'_{cc} = f'_{co} + k_1 f_{le}$, where f_{le} is the equivalent lateral pressure on a square column. The f_{le} is obtained from the equation $f_{le} = k_2 f_l$, while the coefficient $k_1 = 6.7\ (f_{le})^{-0.17}$ and the lateral pressure reduction coefficient $k_2 = 0.26\ [(b_c/s)\ (b_c/s_l)\ (1/f_l)]^{0.5}$.

Triaxial test data from Haider, *et al.* [23] was used to modify the k_1 value (Figure 6(a)). Data processing and non-linear regression analysis produced the following k_1 value:

$$k_1 = 6.8(f_l)^{-0.18} \tag{7}$$

In a square column, the lateral pressure is not uniform, so a coefficient k_2 is needed to reduce the average pressure f_l. A value of k_2 close to *1* indicates that the confinement effectiveness is enhanced. To determine the k_2 value, regression analysis of experimental data was carried out with various influencing variables.

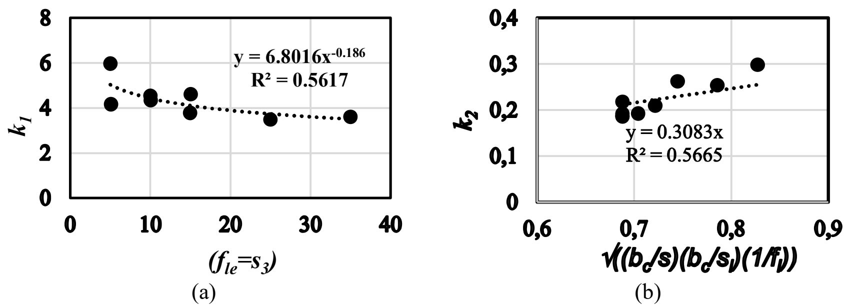

Figure 6 (a) Relationship between lateral pressure f_l and k_1 from research data [23], (b) relationship between parameter k_2 and non-dimensional parameter $[(b_c/s)(b_c/s_l)(1/f_l)]^{0.5}$.

The variables that affect k_2 are tie spacing s, longitudinal reinforcement spacing s_l, width of confined concrete b_c, and lateral pressure f_l. Figure 7(b) depicts the relationship between these variables and k_2.

Based on regression analysis, the relationship between k_2 and the variables that influence it is obtained:

$$k_2 = 0.3\sqrt{\left(\frac{b_c}{s}\frac{b_c}{s_l}\frac{1}{f_l}\right)} \tag{8}$$

Thus, the strength of reinforced concrete can be written as follows:

$$f'_{cc} = f'_{co} + k_1 f_{le} \tag{9}$$

where

$$f_{le} = k_2 f_l \tag{10}$$

$$f_l = \frac{A_{sh} f_{yh}}{s b_c} \tag{11}$$

Verification of Eq. (9) was carried out on test data from Albitar, *et al.* [24], Elchalakani, *et al.* [25], Hussein *et al.* [26], Ganeshan N., *et al*. [8], Sujatha [27], and Saranya, *et al.* [28]. Evaluation was done at $r = f'_{cc\ pred.}/f'_{cc\ exp}$. The results of data processing obtained a coefficient of variation (COV) of 7.96% (Figure 7). A COV below 10% is an acceptable value for compliance [29]. Therefore, the proposed analytical model of confined concrete strength f'_{cc} is suitable.

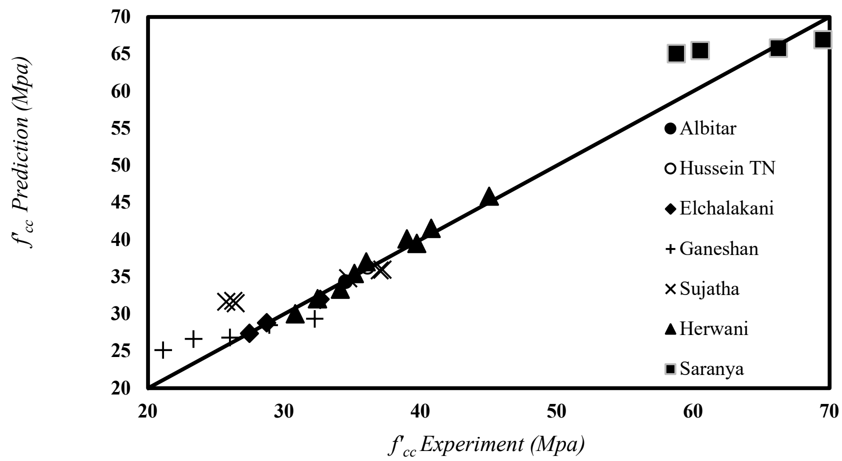

Figure 7 Comparison of the proposed f'_{cc} versus the experimental results.

Substitution of Eq. (9) into Eq. (1) produces strength enhancement K of the confined geopolymer concrete as follows:

$$K = \frac{f'_{cc}}{f'_{co}} = 1 + \frac{k_1 f_{le}}{f'_{co}} \quad (12)$$

The equations of strength enhancement for the confined concrete model proposed by previous researchers are shown in Table 5.

Comparison of the model's and the experimental results were expressed as coefficient of variation. The proposed model was appropriate and suitable, with a COV value of 8.45%. The Saatcioglu & Razvi model can still be applied to GPC concrete columns. Meanwhile, the Giasuddin and Iswandi & Pantazopaolo models are not suitable for square GPC columns, because the developed model is based on active confinement of circular columns. Similarly, the Cusson & Paultre model cannot be used to predict the confined geopolymer concrete strength (f'_{cc}). The developed model is only suitable for high strength concrete.

Table 5 Analytical equation of strength enhancement (K) for confined concrete model.

Researcher	Equations	Remark	COV (%)
Saatcioglu & Razvi [20]	$K=\frac{f'_{cc}}{f'_{co}}=1+\frac{k_1 f_{le}}{f'_{co}}$ $k_1=6.7(f_{le})^{-0.17}$ $f_{le}=k_2 f_l$ $k_2=0.26\sqrt{\left(\frac{b_c}{s}\frac{b_c}{s_l}\frac{1}{f_l}\right)}$	Square column with equivalent lateral pressure parameter	7.56
Cusson & Paultre [30] Legeron & Paultre [31]	$K=\frac{f'_{cc}}{f'_c}$ $=1+2.4\left(\frac{f'_{le}}{f'_{co}}\right)^{0.7}$	Square column of PCC with axial concentric loads	13.71
Imran & Pantazoupoulou [32]	$K=\frac{f'_{cc}}{f'_c}$ $=\left[\frac{f'_2}{f'_c}-0.021\right]+$ $\sqrt{1.043+10.571\frac{f'_2}{f'_c}}$	Triaxial test of PCC	18.35
Giasuddin [23]	$K=\frac{\sigma_1}{f'_c}$ $=1+3.3\left(\frac{\sigma_3}{f'_c}\right)^{0.8}$	Triaxial test of GPC	16.68
Proposed	$K=\frac{f'_{cc}}{f'_{co}}=1+\frac{k_1 f_{le}}{f'_{co}}$ $k_1=6.8(f_{le})^{-0.19}$ $f_{le}=k_2 f_l$ $k_2=0.3\sqrt{\left(\frac{b_c}{s}\frac{b_c}{s_l}\frac{1}{f_l}\right)}$	Square column of GPC with axial concentric loads	8.45

A comparison of the K_{exp} and K_{pre} confined concrete models is shown in Figure 8. The Giasuddin, Iswandi & Pantazopaolo, and Cusson & Paultre models generally appear to overestimate. Meanwhile, the Saatcioglu & Razvi model tends to underestimate. The proposed model produced a K value that was close to the experimental results.

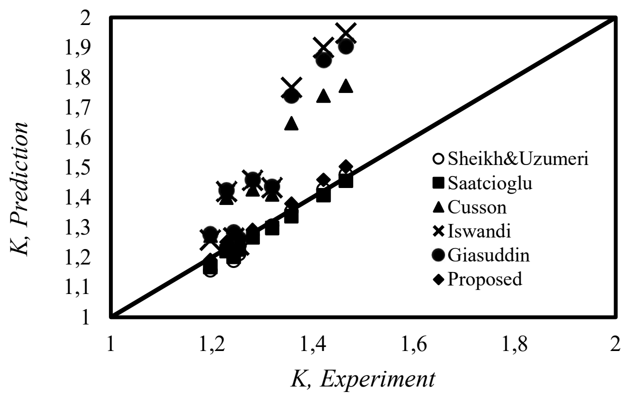

Figure 8 Comparison of $K_{exp.}$ against $K_{pred.}$ confined geopolymer concrete models.

4 Conclusion

In general, the effect of increasing the concrete compressive strength on a column structure increases the confined concrete strength (f'_{cc}) but reduces strength enhancement (K), ductility (μ), and confinement effectiveness index (I_c). The compatibility of concrete and reinforcing steel as well as the configuration of the reinforcing bars contribute to achieving optimal ductility and confinement effectiveness index values.

Increasing tie spacing on the column structure reduced the strength enhancement, ductility, and confinement effectiveness index of confined geopolymer concrete columns. Lateral force due to concrete core expansion was not fully resisted by tie steel bars, causing buckling of the longitudinal reinforcement and concrete crushing.

The proposed equations for the compressive strength of confined geopolymer concrete f'_{cc} (Eq. (9)) and strength enhancement K (Eq. (12)) could predict confined geopolymer concrete compressive strength (f'_{cc}) close to the experimental results, so they are suitable.

Acknowledgments

The authors wish to express their gratitude and sincere appreciation to the Structural and Materials Laboratory Institut Teknologi Bandung, and the Directorate General of Higher Education, Ministry of National Education, the Republic of Indonesia for financing this research work through the Competitive Research Program.

Nomenclature

A_{sh}, A_{sl}	=	Total area of lateral and longitudinal reinforcement
A_c, A_{ch}	=	Total area of concrete core of the confining steel measured center to center
f'_c	=	Compressive strength of cylinder concrete specimen
f'_{cc}, f'_{co}	=	Peak stress of confined and unconfined concrete
f'_l, f'_2	=	Average lateral pressure of confined concrete
f'_{le}	=	Effective confinement pressure at peak load
f'_{sh}	=	Lateral steel stress at peak load
f_y	=	Yield stress of steel reinforcement
h_c, b_c, d_c	=	Width of concrete core measured center to center of the confining steel
k_e	=	Coefficient of effectiveness of confinement geometric
k_1	=	Lateral pressure coefficient as a function of the Poisson ratio
k_2	=	Coefficient for reducing average lateral pressure
P_o	=	Theoretical loads
P_{max}	=	Experimental maximum loads
S	=	Spacing of confining steel measured center to center of the steel
S'	=	Net spacing of confining steel measured face to face of the steel
w_i	=	Face-to-face distance of longitudinal reinforcement
ε_1, ε_{85}	=	Axial strain at peak stress and 85% peak stress
ρ_{exp}	=	Experimental area of lateral reinforcement
ρ_{ACI}	=	Area of lateral reinforcement based on ACI code

References

[1] Herwani, Pane I., Imran I. & Budiono B., Compressive *Strength of Fly Ash-based Geopolymer Concrete with a Variable of Sodium Hydroxide (NaOH) Solution Molarity*, Matec Web of Conferences, **147** (01004), 2018.

[2] Simatupang, P.H., Imran, I., Pane, I. & Sunendar, B., *On the Development of a Nomogram for Alkali Activated Fly Ash Material (AAFAM) Mixtures*, Journal of Eng. Technol. Sci., **47**(3), pp. 231-249, Aug. 2015.

[3] Hardjito, D., Wallah, S.E., Sumajouw, D.M.J. & Rangan, B.V., *On the Development of Fly Ash-Based Geopolymer Concrete*, ACI Materials Journal, **101**(6), pp. 467-472, Nov.-Dec. 2004.

[4] Duxson, P., Fernández-Jiménez, A., Provis, J.L., Lukey, G.C., Palomo, A. & Van Deventer, J.S.J., *Geopolymer Technology: The Current State of the Art*, Journal of Materials Science. **42**(9), pp. 2917-2933, May 2007.

[5] Ma, C.K., Awang, A.Z. & Omar, W., *Structural and Material Performance of Geopolymer Concrete: A Review*, Construction and Building Materials, 186(), pp. 90-102, Jul. 2018.

[6] Balamuralikrishnan, R. & Saravanan, J., *Effect of Addition of Alccofine on the Compressive Strength of Cement Mortar Cubes*, Emerging Science Journal, **5**(2), pp.155-170, Apr. 2021.

[7] Ganesan, N., Abraham. R., Deepa Raj, S. & Sasi, D., *Stress–strain Behaviour of Confined Geopolymer Concrete*, Construction and Building Materials, **73**, pp. 326-331, 2014.

[8] Ganesan, N., Abraham, R. & Deepa Raj, S., *Experimental and Analytical Investigations on Geopolymer Concrete Columns under Repeated Axial Compression*, Asian Journal of Civil Engineering, **16**(5), pp. 651-662, 2015.

[9] Muslikh, Anggraini, N.K., Hardjito D. & Antonius, Behavior *of Geopolymer Concrete Confined by Circular Hoops*, Matec Web of Conferences, **159** (01018), 2018.

[10] Sumajouw, D.M.J., Hardjito, D., Wallah, S.E. & Rangan, B.V., *Fly Ash-based Geopolymer Concrete: Study of Slender Reinforced Columns*, Journal of Materials Science, **42**, pp. 3124-3130, Jun 2006.

[11] Rahman M.M. & Sarker P.K., *Geopolymer concrete columns under combined axial load and biaxial bending*, Proceedings of the Concrete Conference, October, Perth, Australia, 2011.

[12] Sujatha, T., Kannapiran, K. & Nagan, S., *Strength Assessment of Heat Cured Geopolymer Concrete Slender Columns*, Asian Journal of Civil Engineering, **13**(5), pp. 635-646, 2012.

[13] Nhabih. H.T., Hussein., A.M. & Salman., M.M., *Study a Structural Behavior of Eccentrically Loaded GFRP Reinforced Columns Made of Geopolymer Concrete*, Civil Engineering Journal, **6**(3), pp. 563-575, Mar. 2020.

[14] Nguyen, P.D., Dang, V.H., Vu, N.A. & Eduardovich, P.A., *Long-term Deflections of Hybrid GFRP/Steel Reinforced Concrete Beams under Sustained Loads*, Civil Engineering Journal, **6**(special issues), pp. 1-11, 2020.

[15] Kristianto, A., Imran, I., Suardjana, M. & Pane, I., *Confinement of Reinforced-Concrete Columns with Non-Code Compliant Confining Reinforcement Plus Supplemental Pen-Binder*, Journal of Engineering Technology & Science, **44(**3), pp. 220-237, Oct. 2012.

[16] Saatcioglu, M. & Razvi, S.R., *Strength and Ductility of Confined Concrete*, ASCE Journal of Structural Engineering, **118**(6), pp. 1590-1607, June 1992.

[17] Sheikh, S.A. & Uzumeri, S.M., *Strength and Ductility of Tied Concrete Column*, Proceedings, ASCE, **106**(5), pp. 1079-1102, May 1980.

[18] ASTM Committee C09.24, *Standard Specification for Coal Fly Ash and Raw or Calcined Natural Pozzolan for Use in Concrete (C618-15)*, ASTM International, USA, 2015.

[19] Antonius, A. & Imran, I., *Experimental Study of Confined Low-, Medium- and High-Strength Concrete Subjected to Concentric Compression*, Journal of Eng. Technol. Sci., **44**(3), pp. 252-269, Oct. 2012.

[20] Saatcioglu, M. & Razvi, S.R., *Displacement-Based Design of Reinforced Concrete Columns for Confinement*, ACI Structural Journal, **99**(1), pp. 3-11, Jan.-Feb. 2002.
[21] Paultre, P. & Legeron, F., *Confinement Reinforcement Design for Reinforced Concrete Columns*, ASCE Journal of Structural Engineering, **134**(5), pp. 738-749, May 2008.
[22] Richart, F.E., Brandtzaeg, A. & Brown, R.L., *The Failure of Plain and Spirally Reinforced Concrete in Compression*, Univ. of Illinois Bulletin, **XXVI**(31), 190, 1929.
[23] Haider, G.M., Sanjayan, J.G. & Ranjith, P.G., *Complete Triaxial Stress–strain Curves for Geopolymer*, Construction and Building Materials, **69**, pp. 196-202, 2014.
[24] Albitar, M., Ali, M.S.M. & Visintin, P., *Experimental Study on Fly Ash and Lead Smelter Slag-based Geopolymer Concrete Columns*, Construction and Building Materials, **141**, pp. 104-112, 2017.
[25] Elchalakani, M., Dong, M., Karrech, A., Li, G., Ali, M.S.M. & Yang, B., *Experimental Investigation of Rectangular Air-Cured Geopolymer Concrete Columns Reinforced with GFRP Bars and Stirrups*, Journal of Composites for Concrete, **23**(3), 04019011, 1-11, Feb. 2019.
[26] Nhabih, H.T., Hussein, A.M. & Salman, M.M., *Study a Structural Behavior of Eccentrically Loaded GFRP Reinforced Columns Made of Geopolymer Concrete*, Civil Engineering Journal, **6**(3), pp. 563-575, Mar. 2020.
[27] Sujatha, T., *Behaviour and Strength Assessment of Flyash Based Geopolymer Concrete Columns*, PhD Dissertation, Faculty of Civil Engineering., Anna University, Chennai, India, 2012.
[28] Saranya, P., Nagarajan, P. & Shashikala, A.P., *Behaviour of GGBS-dolomite Geopolymer Concrete Beam-column Joints under Monotonic Loading*, Structures, **25**, pp. 47-55, Feb. 2020.
[29] Girgin, Z.C., Arioglu, N. & Arioglu, E., *Evaluation of Strength Criteria for Very-High-Strength Concrete under Triaxial Compression*, ACI Structural Journal, **104**(3), pp. 278-284, May.2007.
[30] Cusson, D. & Paultre, P., *Stress-Strain Model for Confined High-Strength Concrete*, Journal of Structural Engineering, **121**(3), pp. 468-477, Mar. 1995.
[31] Legeron, F. & Paultre, P., *Uniaxial Confinement Model for Normal-and High-Strength Concrete Columns*, Journal of Structural Engineering, **129**(2), pp. 241-252, Feb. 2003.
[32] Imran, I. & Pantazopoulou, S.J., *Plasticity Model for Concrete under Triaxial Compression*, Journal of Engineering Mechanics ASCE, **127**(3), pp. 281-290, Mar. 2001.